JACS
JOURNAL OF THE AMERICAN CHEMICAL SOCIETY
Article
pubs.acs.org/JACS

Collisions of Sodium Atoms with Liquid Glycerol: Insights into Solvation and Ionization

Justin P. Wiens and Gilbert M. Nathanson*

Department of Chemistry, University of Wisconsin-Madison, Madison, Wisconsin 53706, United States

William A. Alexander*

Department of Chemistry, The University of Memphis, Memphis, Tennessee 38152, United States

Timothy K. Minton*

Department of Chemistry and Biochemistry, Montana State University, Bozeman, Montana 59717, United States

Sankaran Lakshmi and George C. Schatz*

Department of Chemistry, Northwestern University, Evanston, Illinois 60208, United States

ABSTRACT: The reactive uptake and ionization of sodium atoms in glycerol were investigated by gas−liquid scattering experiments and ab initio molecular dynamics (AIMD) simulations. A nearly effusive beam of Na atoms at 670 K was directed at liquid glycerol in vacuum, and the scattered Na atoms were detected by a rotatable mass spectrometer. The Na velocity and angular distributions imply that all impinging Na atoms that thermally equilibrate on the surface remain behind, likely ionizing to e^- and Na^+. The reactive uptake of Na atoms into glycerol was determined to be greater than 75%. Complementary AIMD simulations of Na striking a 17-molecule glycerol cluster indicate that the glycerol hydroxyl groups reorient around the Na atom as it makes contact with the cluster and begins to ionize. Although complete ionization did not occur during the 10 ps simulation, distinct correlations among the extent of ionization, separation between Na^+ and e^-, solvent coordination, and binding energies of the Na atom and electron were observed. The combination of experiments and simulations indicates that Na-atom deposition provides a low-energy pathway for generating solvated electrons in the near-interfacial region of protic liquids.

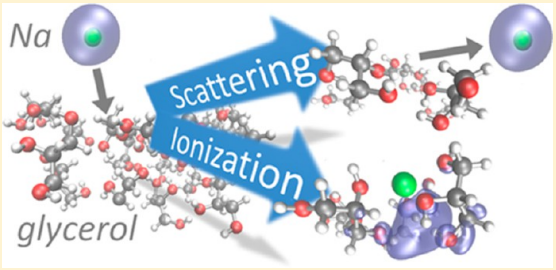

INTRODUCTION

The solvated electron, e_s^-, is a fascinating species both structurally and dynamically,[1−4] and its high reduction potential makes it a powerful reagent in solution.[5−7] Solvated electrons may be generated from high-energy sources[5−7] utilizing megavolt electrons, X-rays, and γ rays and from lower-energy techniques that rely on photodetachment from anions and neutral molecules.[2,3,8−10] They may also be generated at low energies by alkali atom[11] or electron attachment to solvent clusters.[2] There exists a large body of kinetic and mechanistic data for reactions of e_s^- in bulk water,[5,12] ammonia,[13] and alcohols[14] as well as in water clusters,[15,16] which has been extended recently to studies of electron solvation in the interfacial region of liquid water.[9,17−21]

A potentially gentle method for producing solvated electrons at or near the surface of a protic liquid is the gas-phase deposition of sodium atoms, which should rapidly ionize into Na^+ and e_s^-. An analogous technique was employed by Buck and by Kang and their co-workers to investigate solvation and reactions of Na atoms in clusters[11,22,23] and on ice,[24,25] respectively. We recently used this approach to explore reactions initiated by collisions of Na atoms with liquid glycerol, $DOCD_2CD(OD)CD_2OD$, at 287 K.[26] These studies revealed gas-phase products (D, D_2, D_2O, and glycerol open- and/or closed-shell fragments) consistent with e_s^- reactions with polyalcohols, indicating that the accommodated Na atoms likely formed Na^+ and e_s^-.[1,6,14,26,27] Our most remarkable finding was that the deuterium atoms are generated close enough to the surface that 43% of these D atoms escape into vacuum before they can react with solvent glycerol molecules. The production of D atoms by $e_s^- + C_3D_5(OD)_3 \rightarrow D + C_3D_5(OD)_2O^-$ was estimated to occur within a depth of only 50 Å or 10 glycerol layers.

We chose glycerol not only because its low vapor pressure (4×10^{-5} Torr at 287 K[28]) makes it amenable to scattering

Received: October 16, 2013
Published: December 17, 2013

   dx.doi.org/10.1021/ja4106144 | J. Am. Chem. Soc. 2014, 136, 3065−3074

experiments in vacuum but also because of the diverse chemistry that e_s^- exhibits in alcohols.[1,6,14,26,27] In the present work, we extended our studies to identify the types of gas–surface collisions that promote Na-atom reaction and those that lead to complementary nonreactive scattering. To provide microscopic insight into the fate of Na atoms that ionize, we performed ab initio molecular dynamics (AIMD) simulations that follow the Na atom as it begins to form e_s^- and Na^+ at the surface of a 17-molecule cluster representative of the surface of glycerol.

Our AIMD simulations are modeled after those of Jungwirth and co-workers, who tracked the ionization of a Na atom striking a 32-molecule water cluster.[29] They observed increasing electron delocalization and binding over 1.5 ps as the water molecules reoriented to solvate the emerging Na^+ and e_s^- ion pair. The simulations described below show that these solvent motions can be more diverse in glycerol because of the presence of both polar (OH) and nonpolar (CH_2 and CH) groups. Experiments by Mostafavi and co-workers, however, revealed that these nonpolar groups do not substantially inhibit solvation. They showed that electrons generated by solvent photoionization relax 3 times more quickly in pure glycerol (~10 ps at 333 K) than in propanediols, despite glycerol's 2-fold higher viscosity.[30] This fast relaxation was attributed to the high density of glycerol OH groups, which create configurations that rapidly stabilize the ejected electron.

The thermodynamics of Na ionization in glycerol have not been measured, but in water the process $Na(g) \rightarrow Na^+(aq) + e_s^-(aq)$ is estimated to be exothermic by approximately 70 kJ mol^{-1} at 298 K.[31] This reaction may be decomposed into separate steps involving gas-phase ionization, ion solvation, and electron solvation: $Na(g) \rightarrow Na^+(g) + e^-(g)$, endothermic by 499 kJ mol^{-1};[32] $Na^+(g) \rightarrow Na^+(aq)$, exothermic by ~463 kJ mol^{-1}; and $e^-(g) \rightarrow e_s^-$, exothermic by ~109 kJ mol^{-1}.[31,33−35] The much larger hydration enthalpy for Na^+ than for e_s^- emphasizes that solvation of the Na cation is essential for the exothermic dissolution and ionization of Na atoms in water. Despite this constraint, our simulations indicate that partial ionization to a Na^+ e_s^- complex begins almost immediately upon contact of Na with glycerol and could potentially be complete within tens of picoseconds. The influence of Na^+ on electron solvation has been investigated explicitly by comparing photoionization of Na-doped water and alcohol clusters[11,23,36] with that of the analogous anionic clusters containing just the electron.[2,3,37] These studies revealed that the ionization energies of small Na-doped clusters are ≥100 kJ mol^{-1} higher than those of the anionic clusters, implying that the cation stabilizes the electron when they are in close contact.[38−40]

The dynamics of solvation and ionization start with the approach of the neutral alkali atom to the surface of the liquid. In the studies described here, we investigated these processes experimentally by characterizing the collisions that enable Na atoms to react and theoretically by following the Na atom as it becomes surrounded by glycerol OH groups and begins to ionize. While our simulations did not show complete ion separation (as a result of practical computational limitations), they nevertheless provide detailed insight into the solvation and partial ionization of a Na atom during the initial stages of its encounter with a model protic liquid.

EXPERIMENTAL METHODS

The experiments were performed using a crossed molecular beams apparatus modified for gas–surface scattering (Figure 1).[41,42] A nearly

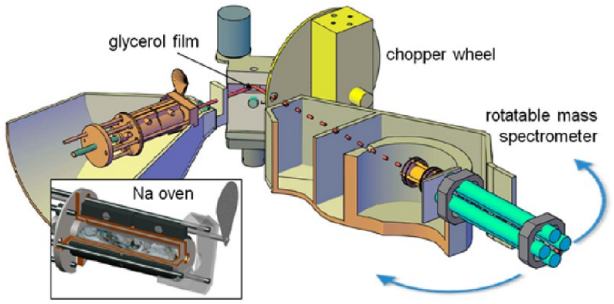

Figure 1. Diagram of the Na oven, liquid reservoir and wetted wheel, and differentially pumped rotatable mass spectrometer.

effusive beam of Na atoms was directed at a continuously refreshed liquid glycerol film. The scattered Na atoms were chopped into 20 μs pulses by a spinning slotted wheel; the pulses then traveled 29.4 cm to an electron-impact ionizer, where their arrival times were recorded as a time-of-flight (TOF) spectrum by a triply differentially pumped mass spectrometer. By rotation of the liquid reservoir and the mass spectrometer about the same axis, the TOF distributions were monitored at different incident angles, θ_{inc}, and final (exit) angles, θ_{fin}. In the subsections below, we describe the glycerol isotopes, liquid reservoir, and sodium oven used in the experiments.

Glycerol Liquid Reservoir and Interaction Region. Three glycerol solutions were used in the experiments. Glycerol [$C_3H_5(OH)_3$, denoted as h_8-gly] was obtained from Sigma-Aldrich, and fully deuterated glycerol [$C_3D_5(OD)_3$; d_8-gly] was obtained from Cambridge Isotopes. Partially deuterated glycerol [$C_3H_5(OD)_3$; d_3-gly, 80% and 96% deuteration] was made by iterative distillation of h_8-gly with D_2O. All of the glycerol samples were degassed to below 20 mTorr and then poured into the reservoir in the scattering chamber. A vertical liquid film was produced by rotating a 5.0 cm diameter glass wheel through a 19 mL glycerol reservoir[43] maintained at T_{liq} = 287 K. The film was continuously scraped by a sapphire plate, leaving behind a fresh 100 μm thick film on the wheel, which was then exposed to the Na-atom beam through a 1.2 cm high × 1.8 cm wide window in the reservoir. For fixed-angle experiments at $\theta_{inc} = \theta_{fin} = 45°$, the incident Na beam projected a 0.40 cm × 0.56 cm elliptical spot on the surface. The wheel rotation frequency was 0.25 Hz, resulting in a Na beam exposure time of 0.19 s.

Na-atom angular distributions were measured by narrowing the beam so that it projected 0.11 cm × 0.28 cm and 0.14 cm × 0.28 cm spots on the surface at θ_{inc} = 45° and 60°, respectively. This spatial narrowing reduced the exposure times to 0.06 and 0.09 s for θ_{inc} = 45° and 60°, respectively. The angular distributions were recorded in 5° increments from θ_{fin} = 22° to 67° for θ_{inc} = 45° and from 7° to 62° for θ_{inc} = 60°.

Sodium Oven and Incident Beam Characteristics. The horizontally mounted oven was machined from stainless steel and consisted of two concentric cylinders heated by barrel heaters (depicted in the inset of Figure 1). Approximately 7 g of Na metal (Aldrich, 99.9%) was inserted into the inner cylinder after the oil-covered bark was scraped from the oxidized Na bars. Residual mineral oil was pumped away by preheating the oven to 470 K in vacuum, which is higher than the Na melting point (371 K). The Na vapor passed through a 3 mm diameter hole in the inner oven and effused from the outer cylinder through a second 3 mm diameter hole. The Na atoms then traveled through a heat shield and two defining apertures before striking the liquid film 8.5 cm from the oven exit.

The Na beam was characterized by directing it into the mass spectrometer. Figure 2 shows a TOF distribution of the Na beam at a typical oven temperature (T_{oven}) of 667 K, recorded at a mass-to-charge ratio (m/z) of 23 (Na^+). This distribution is slightly narrower than a Maxwell–Boltzmann (MB) distribution at T_{oven} = 667 K and is characterized by an average incident energy $\langle E_{inc} \rangle$ = 11.8 kJ mol^{-1} with a full width at half-maximum of 13.4 kJ mol^{-1}. The 0.3 Torr vapor pressure of Na at 667 K yields a Knudsen number (ratio of the mean

dx.doi.org/10.1021/ja4106144 | J. Am. Chem. Soc. 2014, 136, 3065−3074

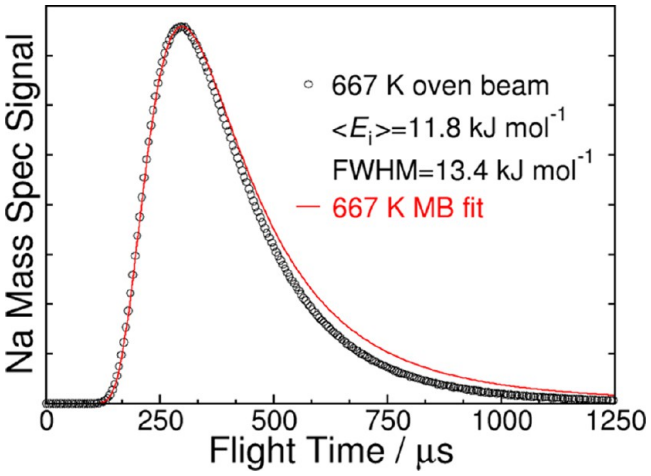

Figure 2. Incident Na beam time-of-flight (TOF) distribution obtained with a 667 K oven temperature. This nearly effusive Na beam is compared with a Maxwell–Boltzmann (MB) distribution at the same temperature.

free path to the orifice diameter) of ∼0.1; this value implies that there were sufficient collisions at the nozzle exit to produce slight deviations from effusive behavior.[44] Na dimers were detected at m/z = 46 in the beam at <1% of the overall beam intensity, but trimers (m/z = 69) could not be observed. At an oven temperature near 667 K, the 7 g Na load provided 8–10 h of usable beam time.

The absolute Na beam flux at 667 K was not measured, but we estimate it to be 1 × 10^{16} cm^{-2} s^{-1} (∼10 monolayers per second) on the glycerol film. During the 0.19 s exposure time, the rotating film was exposed to roughly 4 × 10^{14} Na atoms as it passed by the hole in the liquid reservoir. Accumulation of Na atoms ultimately led to the creation of basic species [$C_3H_5(OH)_2^-$ and OH^- from e_s^- reaction with h_s-gly] and was predicted to produce a ∼0.005 M basic solution over a typical 10 h exposure time before the glycerol sample was replaced.

THEORETICAL METHODS

To gain insight into Na-atom ionization at the glycerol–vacuum interface, we performed ab initio molecular dynamics (AIMD) simulations of a sodium atom impinging on a 17-molecule glycerol cluster carved out of the surface of a box containing 192 glycerol molecules. Bulk liquid glycerol was modeled using the empirical potential developed by Blieck et al.[45] based on the all-atom AMBER force field,[46] which has been shown to give excellent agreement with structural, vibrational, thermodynamic, and diffusion data.[47]

Two preliminary classical MD simulations were performed to create a glycerol cluster for the AIMD simulation with the sodium atom. In the first MD simulation, 64 glycerol molecules were placed in a periodic box and equilibrated at 298 K and 1 atm for 1 ns with a time step of 0.5 ps. The equilibrated density of 1.22 g cm^{-3} agrees well with the experimental value of 1.26 g cm^{-3}. In the second MD simulation, the equilibrated periodic box length of 20 Å was tripled along one direction to include 192 molecules in a 20 Å × 20 Å × 90 Å box that includes a 30 Å vacuum region. This simulation was performed in the *NVT* ensemble at 298 K for 1 ns and provided two 20 Å × 20 Å surfaces from which we could sample interfacial dynamics. Both classical MD simulations were performed using the TINKER package.[48] A 17-molecule cluster was then carved out of one of the interfacial regions of the 192-molecule system, as shown in Figure 3. The surface of the cluster consists predominantly of CH and CH_2 groups with their hydrogen atoms [denoted as H(C)] protruding from the surface, while the hydrogen atoms of the surface hydroxyl groups [H(O)] are each hydrogen bonded to neighboring O atoms, inhibiting their ability to extend into vacuum.[49] This surface composition is consistent with vibrational spectroscopy measurements[50] and is more hydrophobic than in previous calculations using united atoms for CH_2 and CH.[51] We estimate that the fractions of surface atoms are 53% for H(C), 24% for C, 13% for O, and 10% for H(O), with uncertainties of at least 1 part in 10 for each fraction.

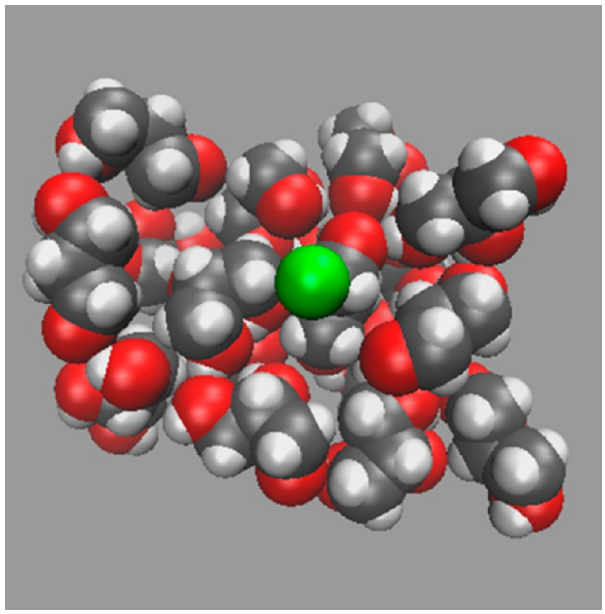

Figure 3. Top view of the surface of the 17-molecule glycerol cluster (C, gray; O, red; H, white). The snapshot was taken at 0 fs with the Na atom (green) traveling toward the surface in a direction normal to the picture.

The scattering simulation was performed by placing a sodium atom 3.4 Å above the surface cluster (depicted in green in Figure 3). The Na atom was then directed at the cluster with an initial translational energy of 2.3 eV (this high value was chosen to accelerate the dynamics, the consequences of which will be discussed later), corresponding to a speed of 44 Å/ps. We then followed the motions of the Na atom and glycerol using AIMD as implemented in the CP2K/QUICKSTEP software.[52] Density functional theory (DFT) with the BLYP exchange–correlation functional, double-ζ valence polarization (DZVP) basis set, and Goedecker–Teter–Hutter (GTH) pseudopotential was employed for these unrestricted, open-shell calculations. Hybrid Gaussian and plane waves (GPW) were used to describe the wave functions and the densities, respectively. The energy cutoff for the plane waves was considered to be 1000 Ry. The whole cluster was placed in a cubic, nonperiodic 30 Å × 30 Å × 30 Å box, and the Poisson equation was treated using a wavelet-based solver. Born–Oppenheimer molecular dynamics (BOMD) was performed in the *NVE* ensemble with an integration time step of 0.5 fs up to a total simulation time of 10 ps. This trajectory required nearly a year of computation time, and we are thus unable to provide information about the behavior of a statistical ensemble.

The Na atom dissipated its excess kinetic energy during ∼500 fs following its collision with the cluster. After this equilibration time, the temperature of the system was found to fluctuate around 270 K, which is close to the experimental glycerol temperature of T_{gly} = 287 K. Among the quantities calculated along the trajectory was the cluster vertical ionization potential (VIP). The VIP was not corrected for the self-interaction energy of the electron. As shown in ref 29 for Na atoms interacting with a water cluster, this term adds a ∼0.5 eV offset to the electron VIPs but does not alter the trends.

EXPERIMENTAL RESULTS AND ANALYSIS

Scattering of Na Atoms. We first monitored the velocity and angular distributions of Na atoms recoiling from the glycerol film and then measured the fraction of impinging Na atoms that reacted with the liquid. The Na atoms were vaporized at T_{oven} ≈ 680 K, corresponding to an average

dx.doi.org/10.1021/ja4106144 | J. Am. Chem. Soc. 2014, 136, 3065–3074

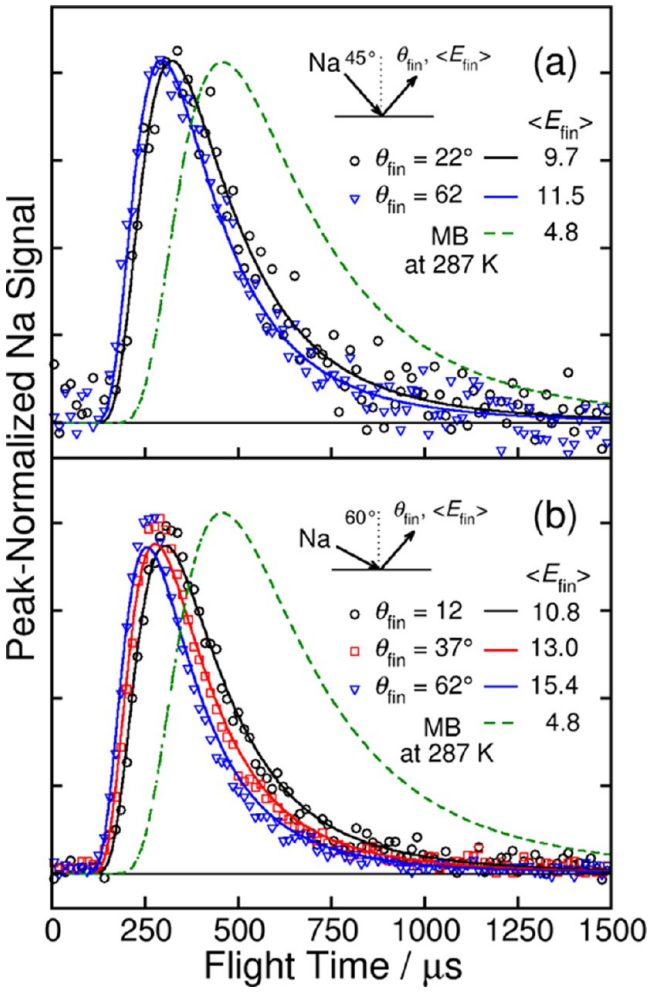

Figure 4. TOF spectra of Na atoms scattered from glycerol at T_{liq} = 287 K at incident angles θ_{inc} of (a) 45° and (b) 60°. The Na oven temperature was 680 K. The solid lines are fits to the data using MB distributions with the indicated average translational energies (in kJ mol^{-1}). These MB curves are used only as convenient fitting functions. The dashed green curve is a MB distribution at T_{liq} expected for thermal desorption of the Na atoms, peak-normalized to the peak of the scattering data.

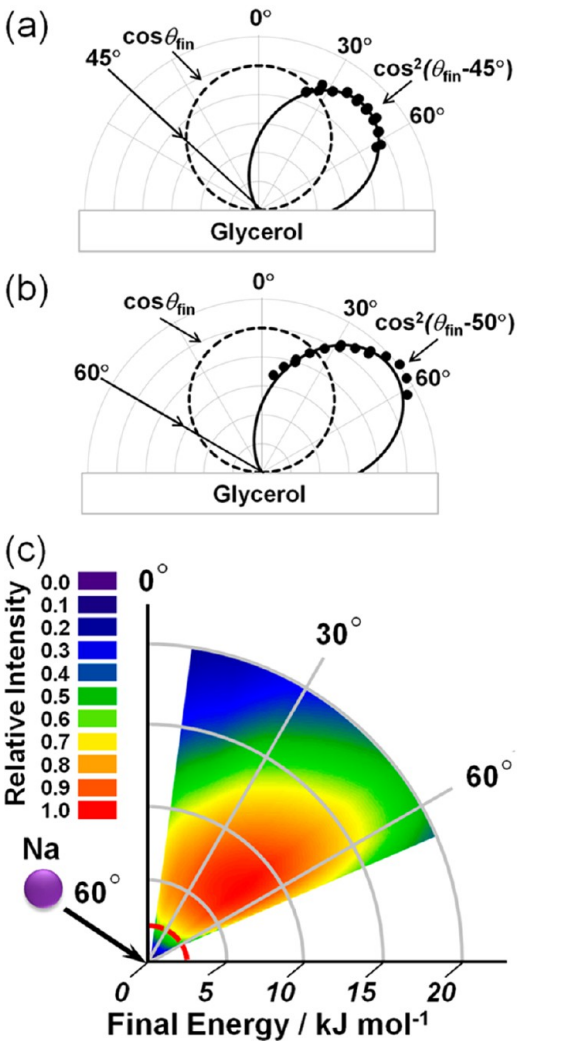

Figure 5. Angular distributions of scattered Na-atom flux for (a) θ_{inc} = 45° from 96% d_3-gly and (b) θ_{inc} = 60° from d_8-gly. (c) Flux contour map of Na atoms scattered from d_8-gly at θ_{inc} = 60°. The red dashed curve near the origin corresponds to $E_{fin} = RT_{liq}$ = 2.4 kJ mol^{-1}, equal to the peak energy of a MB distribution at T_{liq} = 287 K.

collision energy of 12 kJ mol^{-1} ($5.0RT_{liq}$) and a full width at half-maximum of 14 kJ mol^{-1}. Figure 4a shows TOF spectra of the Na atoms after striking the 96% d_3-gly film at T_{liq} = 287 K with θ_{inc} = 45° for exit angles of θ_{fin} = 22° and 62°. Each TOF spectrum was fit with a MB distribution characterized by an average flux-weighted translational energy $\langle E_{fin} \rangle = 2RT_{fit}$. This distribution was chosen only because it provides a useful one-parameter fitting function; the TOF distributions would likely be much narrower if the incident Na beam were mono-energetic. The average recoil energies at θ_{fin} = 22° and 62° are 9.7 and 11.5 kJ mol^{-1}, respectively, indicating that the recoil energy is not constant but increases with exit angle. This trend is even more pronounced at a more grazing impact angle of θ_{inc} = 60°, as shown in Figure 4b, where the average energies of scattered Na atoms from d_8-gly are 10.8, 13.0, and 15.4 kJ mol^{-1} for θ_{fin} = 12°, 37°, and 62°, respectively. In no case do the TOF spectra resemble a MB distribution at the 287 K temperature of the glycerol (for which $\langle E_{fin} \rangle = 2RT_{liq}$ = 4.8 kJ mol^{-1}), as would be expected if the Na atoms had thermally equilibrated at the surface and then desorbed.[53]

The angular distributions at θ_{inc} = 45° and 60° in Figure 5 further indicate that the exiting Na atoms scattered lobularly into the forward direction. These outgoing fluxes were calculated from the TOF distributions at each angle by integrating $N(t)/t$, where t is the flight time. The resulting angular distributions were fit empirically with the functional form $\cos^2(\theta_{fin} - \theta_{peak})$. The two distributions peak near the 45° and 60° specular angles and do not resemble an azimuthally symmetric cosine angular distribution, which would be expected for thermal desorption of equilibrated Na atoms and would instead be greatest at 0°.

Figure 5c combines 13 Na-atom TOF distributions at θ_{inc} = 60° into a flux contour map as a function of final energy and final angle θ_{fin} from 7° to 62°. The most probable energy of a MB distribution at T_{liq} = 287 K (RT_{liq} = 2.4 kJ mol^{-1}) is denoted by the red dashed line near the origin. The sharp contrast between the predicted thermal desorption line and the data implies that thermally equilibrated Na atoms did not desorb from the glycerol film but instead disappeared into the liquid. In this case, Na atoms escaped from the liquid only by recoiling directly from the surface after one or a few bounces.

dx.doi.org/10.1021/ja4106144 | J. Am. Chem. Soc. 2014, 136, 3065−3074

The increase in recoil energy with final angle (Figures 4 and 5) is consistent with impulsive, spherelike collisions between Na atoms and a localized region of the surface comprising different combinations of C, H, and O atoms.[54] In particular, glancing collisions at high impact parameters would be expected to direct the Na atoms into the forward direction, transferring a smaller fraction of their incident energy to the surface. At the smallest deflection geometry of $\theta_{inc} = 60°$ and $\theta_{fin} = 62°$, the average 15.4 kJ mol^{-1} recoil energy actually exceeds the average 11.8 kJ mol^{-1} incident energy. This surprising result implies that higher-energy Na atoms within the broad incident energy distribution (14 kJ mol^{-1} fwhm) preferentially scatter from the surface while lower-energy Na atoms are captured by the liquid.

Na-Atom Reaction Probability. The fraction of incoming Na atoms that react with liquid glycerol was estimated by comparing the Na-atom scattering signal from the glycerol film to that obtained from Na-atom scattering from an inert fluorinated ethylene polypropylene (FEP) Teflon surface at the same exit angle.[55,56] Figure 6 displays the TOF distributions

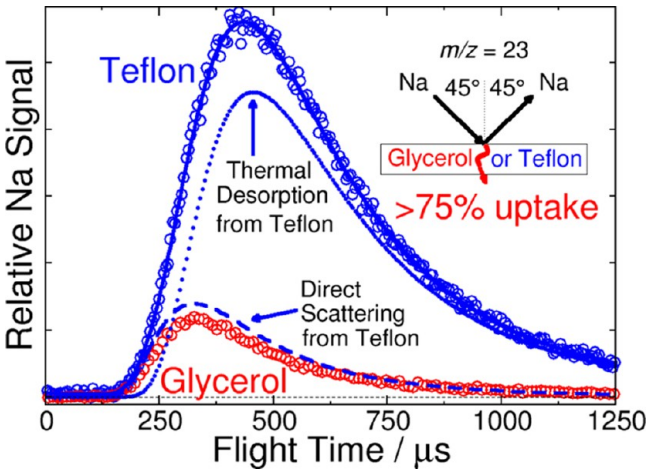

Figure 6. TOF spectra of Na atoms at $T_{oven} = 670$ K scattered from FEP Teflon and from 80% d_3-gly. The dotted blue curve is a MB fit to the Teflon TOF spectrum at $T_{Teflon} = 287$ K assigned to thermal desorption (TD) of equilibrated Na atoms. The difference between the Teflon spectrum and the TD fit is shown by the blue dashed line and is assigned to direct Na-atom scattering; this curve is nearly equal in intensity and shape to that for Na-atom scattering from glycerol. This good overlap suggests that Na atoms that equilibrate on the Teflon surface enter the liquid glycerol film and ionize.

from Na-atom collisions with Teflon (blue) and 80% d_3-gly (red) at $\theta_{inc} = \theta_{fin} = 45°$ and $T_{oven} = 670$ K. Integration of $N(t)/t$ for each spectrum indicated that the scattered Na flux from Teflon was 4.0 ± 1.1 times greater than that from 80% d_3-gly at $\theta_{fin} = 45°$. If the angular distributions from Teflon and glycerol were identical, then the flux ratio measured at $\theta_{fin} = 45°$ would be equal to the ratio of fluxes over all exit angles, and the fraction of Na atoms that reacted with glycerol would be 0.75 ± 0.08. Further analysis below indicates that this 75% reaction probability is a lower limit.

Figure 6 shows that Na-atom scattering from Teflon can be decomposed into two components corresponding to (1) Na atoms that thermally equilibrate with the surface and then desorb in a MB distribution at $T_{liq} = 287$ K (lower velocities and longer arrival times; dotted line), and (2) Na atoms that scatter directly from the surface, obtained by subtracting the MB component from the full TOF spectrum (dashed line at early arrival times). The dominant low-energy MB component is consistent with trapping followed by thermal desorption of the Na atoms. These atoms lose memory of their initial trajectory and desorb in a broad, azimuthally symmetric distribution that is likely to be cosine in shape.[57,58] The Na signal from Teflon measured at $\theta_{fin} = 45°$ therefore represents a much smaller fraction of the outgoing Na atoms than it does for the focused, forward-peaked glycerol distribution, where the signal is largest at 45° (Figure 5a). In this case, the 4:1 ratio of Na-atom fluxes for Teflon and glycerol at $\theta_{fin} = 45°$ is smaller than the ratio integrated over all exit angles, making the 0.75 reaction probability a lower limit. These experiments were performed with 80% d_3-gly, but we observed comparable scattering intensities from all of the glycerol isotopes, suggesting that interfacial OH and OD groups capture Na atoms with similar probabilities. The high (0.75 or greater) reaction probability also implies that the presence of surface CH_2 and CH groups does not significantly impede contact between the Na atom and these surface hydroxyl groups.

Lastly, we note that the higher-energy, direct-scattering component of the Na TOF distribution from Teflon in Figure 6 has nearly the same shape and magnitude as the Na-atom distribution from glycerol. This good overlap supports the interpretation that higher-energy Na atoms in the incident beam scatter directly from the surface of glycerol while those at lower energies equilibrate at the surface and disappear into the liquid.

The absence of thermally desorbing Na atoms from glycerol implies that they begin to ionize into Na^+ and e^- before thermal motions of the surface glycerol molecules propel them back into the gas phase. This conjecture is supported by the simulation described below, which indicates that ionization begins in the first picosecond of contact with the outermost surface glycerol molecules. Previous AIMD simulations of Na-atom collisions with water clusters also corroborate this rapid interfacial ionization and show that water molecules rearrange to stabilize the evolving Na_s^+ and e_s^- by orienting their OH groups toward the charged species.[29] Hydroxyl group reorientation appears to be more complex in glycerol because of the distinct interactions of the Na atom with alkyl and OH groups in the cluster.

AB INITIO MOLECULAR DYNAMICS SIMULATIONS OF SODIUM-ATOM IONIZATION

A 10 ps AIMD simulation was performed to gain insight into the solvation and ionization of a Na atom as it impinges onto a 17-molecule glycerol cluster that mimics the surface of liquid glycerol. As described above, the initial surface configuration was obtained from the previously prepared glycerol cluster. In order to facilitate quick contact with the surface, the Na atom was placed 3.4 Å above the surface with an initial translational energy of 220 kJ mol^{-1} (2.3 eV), which is much higher than the 12 kJ mol^{-1} (0.12 eV) collision energy used in the experiment. As shown below, most of this 2.3 eV energy is dissipated within 500 fs of the collision.

Figure 7 shows six snapshots of the simulation from 0 to 10 ps. The dark-blue envelope in each panel corresponds to an isodensity surface value of 0.001 electron per cubic bohr (isovalue, as implemented in ref 59) obtained from the spin density distribution. Each panel also lists the fractional ionization of the Na atom (labeled as "% ion"). The 500 fs panel highlights incipient interactions between the Na atom

dx.doi.org/10.1021/ja4106144 | J. Am. Chem. Soc. 2014, 136, 3065−3074

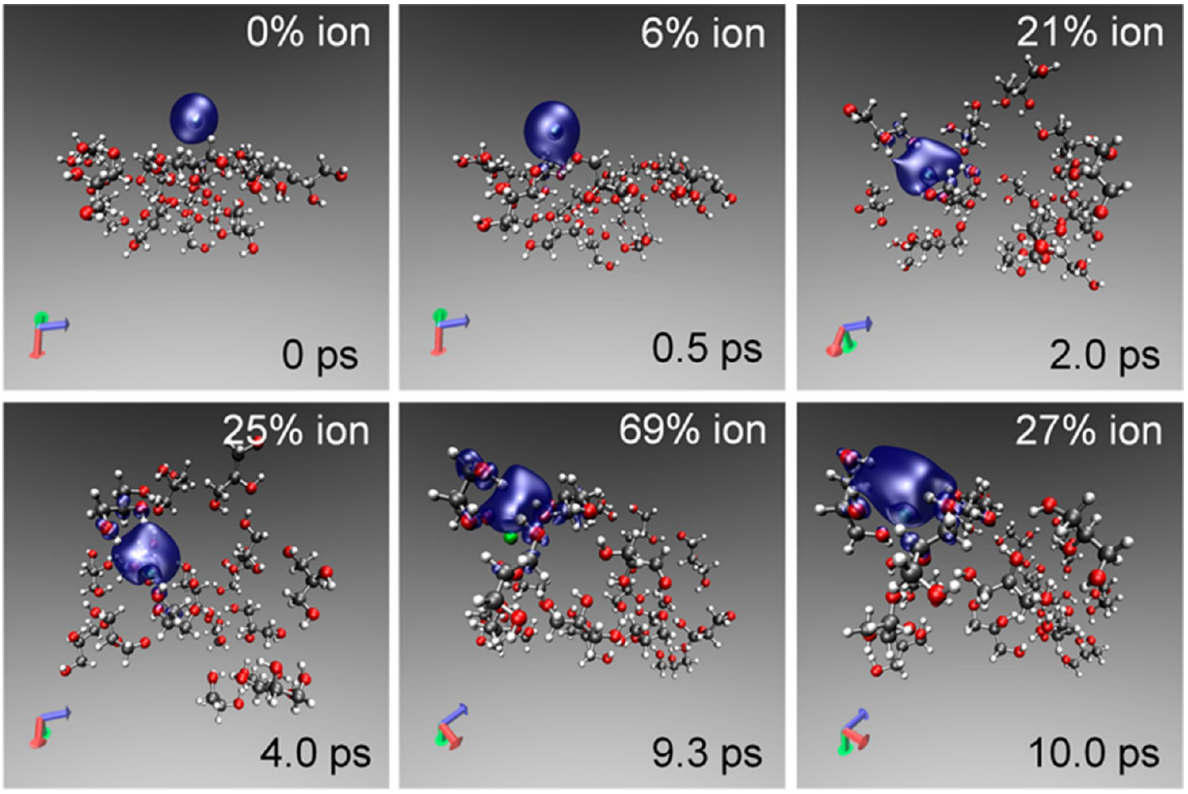

Figure 7. Snapshots of the spin density (blue) of the 3s electron of the Na atom (green) during contact with a 17-molecule glycerol cluster (C, gray; O, red; H, white) at ~270 K. The snapshots were generated by ab initio molecular dynamics calculations at simulation times indicated in the panels. The ionization fraction at each snapshot is listed in the corresponding panel.

and surface OH groups that allow the electron to begin moving from the Na atom to these OH groups. Consistent with previous electron solvation studies in water clusters,[19,29,60] progressively more hydroxyl groups orient around the Na atom as the H(O) atoms form a cavity to enclose the Na 3s electron while O atoms surround the ionizing Na atom (2.0–9.3 ps panels). Ionization reached ~69% at 9.3 ps (and an overall maximum of 78% just before this time).[61] At 10 ps, however, the reorientation of a few glycerol molecules caused Na^+ and e^- to move abruptly toward each other, and the fractional ionization dropped to 27%. Fluctuations on this time scale suggest that complete Na-atom ionization in the 270 K glycerol cluster requires longer than 10 ps. This time appears to be longer than the time scale for ionization of a Na atom at the surface of a 350 K water cluster,[29] as might be expected from the lower temperature of the cluster (270 K) and the longer hydrogen-bond lifetimes in glycerol (tens of picoseconds).[47,62]

We begin a detailed analysis of the trajectory by comparing in Figure 8 the Na-atom kinetic energy (Na KE), the distance from the Na atom to the nearest atom of the glycerol cluster [$r_{(Na-gly)}$], and the Na-atom vertical detachment energy (Na VDE) from the cluster during the first 1000 fs of the trajectory. The Na VDE is a measure of the Na-atom binding energy in the cluster: larger values indicate greater solvation of the atom as it ionizes to form Na^+ and e^-, whereas smaller values indicate a more weakly bound and less ionized Na atom. The Na VDE was determined by removing the Na atom from the cluster while freezing the glycerol molecules in their original configuration; the value was computed as the differences in the potential energies (PE):

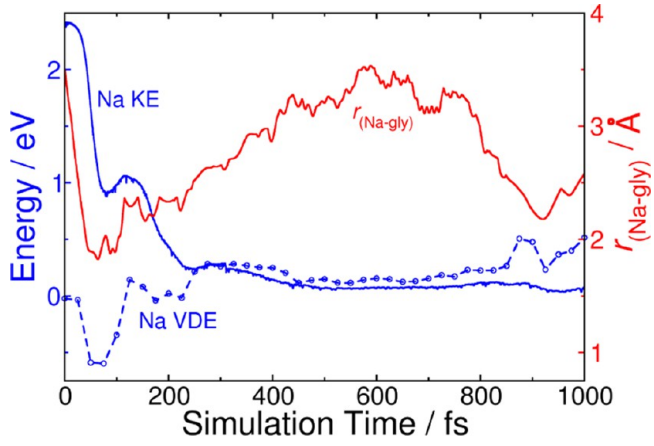

Figure 8. Kinetic energy (Na KE) and vertical detachment energy (Na VDE) of the Na atom and distance between Na and nearest glycerol atom of the cluster [$r_{(Na-gly)}$] for the first 1000 fs of the simulation. The Na KE drops sharply to near-thermal values within 200 fs.

$$\text{Na VDE}(t) = \text{PE}_{\text{Na(g)}} + \text{PE}_{\text{cluster without Na}}(t) - \text{PE}_{\text{cluster with Na}}(t)$$

Figure 8 reveals that the Na VDE is slightly positive for most of the first 1000 fs of the trajectory, which, as shown later, coincides with partial electron transfer from Na to neighboring glycerol molecules. During the first 150 fs, the Na atom loses ~65% of its initial kinetic energy as it collides with protruding alkyl groups and is deflected along the surface. This repulsive interaction is reflected in the negative Na VDE and short Na–glycerol distance during this time. The Na–glycerol distance,

dx.doi.org/10.1021/ja4106144 | J. Am. Chem. Soc. 2014, 136, 3065–3074

$r_{(Na-gly)}$, increases after ~70 fs as the Na atom recoils, but Na–glycerol attractive forces keep Na within 3.5 Å of the surface, and the Na VDE becomes positive after ~120 fs. Following the initial collision, the Na atom moves ~5 Å along the surface during the first 500 fs, losing an additional 25% of its initial kinetic energy. As illustrated in the 0.5 ps panel of Figure 7 and detailed below, this thermalization occurs while the Na atom encounters stabilizing hydroxyl groups, which begin to orient around it. Beyond the first 500 fs, the Na kinetic energy oscillates between 0.05 and 0.2 eV as it thermally equilibrates with the cluster. This low translational energy mimics the 12 kJ mol^{-1} Na incident energy used in the experiment.

We next followed the glycerol molecules as they reoriented to form a solvent cage around the Na atom and ionizing electron. The solvent motions were quantified by counting the numbers of nearest neighbors of particular species present within a 3.0 Å sphere around the Na atom (the coordination numbers, CNs) throughout the simulation. Figure 9a shows that the CNs increase for all atomic species as the Na atom approaches the cluster. Within the first 150 fs, Na reaches its highest coordination with H(C) atoms as it impacts the collision zone. After this initial contact with the surface, all of the CNs decrease because repulsive interactions push the Na atom away from the cluster. Na coordination with CH and CH_2 groups, as represented by the H(C) curve, then remains small throughout the trajectory as the initially hydrocarbon-rich surface adjusts to accommodate the ionizing Na atom, as indicated by increasing coordination between Na and the glycerol H(O) and O atoms. Figure 9b displays the CNs of the electron (i.e., the numbers of atoms within 3.0 Å of the center of the electron density). During the trajectory, the H(O) atoms form a cavity to stabilize and solvate the electron separately from the ionizing Na atom. In both panels, the H(O) and O CNs reach a maximum near 9.3 ps. Because H(O) and O are in close proximity to each other, the CNs of these species track each other as the extent of solvation changes.

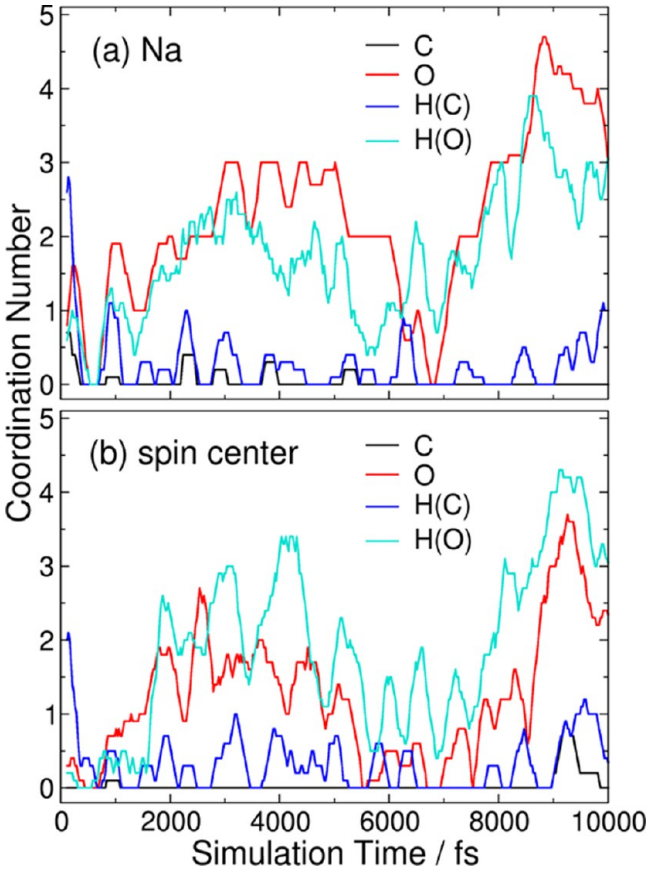

Figure 9. (a) Na-atom and (b) electron coordination numbers (3 Å cutoff) for the C, O, H(O), and H(C) atoms of glycerol as functions of simulation time. The initial coordination with the alkyl groups shifts to coordination with the OH groups after 2 ps and thereafter stays near zero throughout the simulation. The O and H(O) group coordination numbers fluctuate throughout the simulation, increasing to a maximum at 9 ps. The data points are 10-point running averages of the coordination numbers determined every 25 fs.

The ionization process itself may be quantified by analyzing the spin population of the Na atom during solvent reorganization. This population was determined by calculating the Na 3s Mulliken spin density, which equals the fractional electron charge on the Na atom. We have plotted the difference (1 − spin population) in Figure 10 because this quantity directly measures the extent of ionization of the Na atom. Figure 10 shows that the extent of ionization fluctuates throughout the trajectory as the hydroxyl and alkyl groups reorient in the cluster. To explore the origin of these fluctuations, we also compare the changes in the spin population with the O coordination number around the spin center (red line in Figure 10). The good overlap throughout the trajectory is also found for the other H(O) and O coordination numbers in Figure 9. These parallel trends suggest that the extent of ionization is correlated with the positions of the H(O) and O atoms neighboring the incipient Na^+ and e_s^-. The sharp transition near 9.3 ps, however, most likely involves subtle changes in the hydrogen-bonding network far from the ionization region as well.[63] In particular, the 9.300 ps snapshot in Figure 7 corresponds to 69% ionization, just beyond the maximum ionization of 78% at 9.283 ps. This distinct change occurs despite little motion of the alkyl and hydroxyl groups in the first solvation shell around the Na atom.

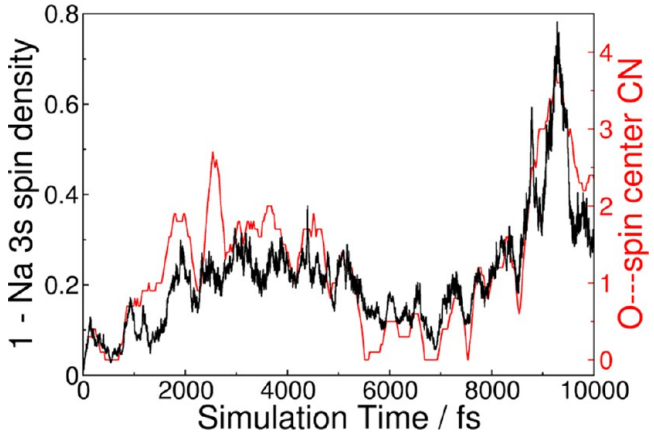

Figure 10. Plot of the difference (1 − Na 3s spin population) vs simulation time (black). This difference measures the extent of Na-atom ionization. Also shown is the glycerol O-atom coordination number around the spin center (red), which also peaks near 9.3 ps.

Figure 10 further shows that the extent of ionization drops from its maximum of 78% near 9.3 ps to 27% at the end of the simulation (10 ps). Complete ionization of the Na atom (with the formation of well-separated Na^+ and e_s^-) was not observed, most likely because of the small cluster size and limited simulation time. There was also no evidence for reactions such

dx.doi.org/10.1021/ja4106144 | J. Am. Chem. Soc. 2014, 136, 3065–3074

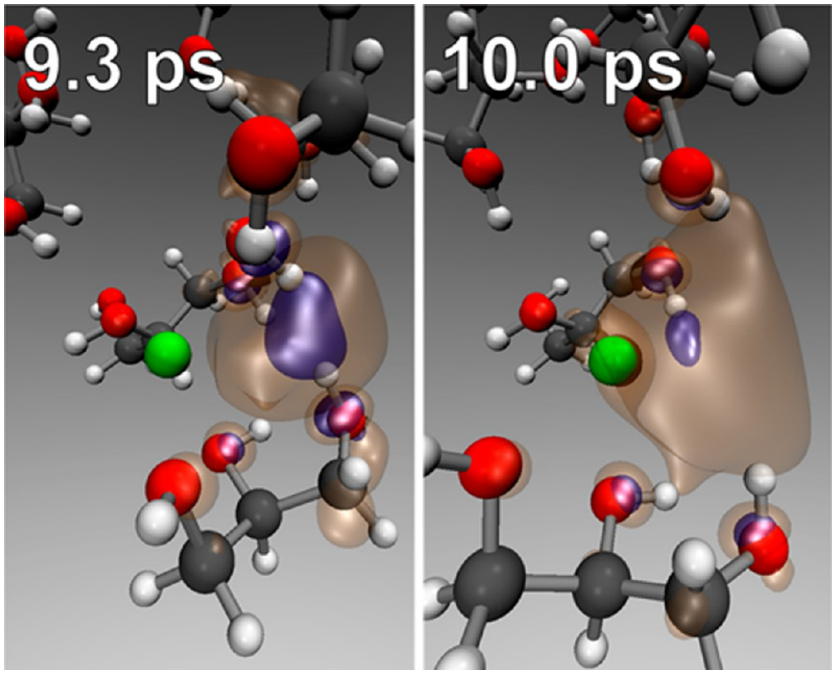

Figure 11. Zoomed-in views of the spin density isosurfaces from the same vantage point at 9.3 ps and 10.0 ps. The dark-blue surfaces correspond to an isodensity of 0.006 and the gold surfaces to an isodensity of 0.001 electron per cubic bohr. Comparison of the snapshots indicates that the Na atom (green) is more separated from the electron density and the electron density is more localized within the hydroxyl-stabilized solvation cavity at 9.3 ps than at 10.0 ps.

as $e^- + C_3H_5(OH)_3 \rightarrow H + C_3H_5(OH)_2O^-$ over this time period. As discussed in ref 64, this reaction likely occurs on a microsecond time scale.

Detailed views of the sharp transition in ionization from 9.3 to 10.0 ps are compared in Figure 11, where the larger gold envelope denotes a surface of 0.001 electron density (isovalue of 0.001) and the smaller dark-blue "kernel" denotes a surface of 0.006 electron density. The snapshot at 9.3 ps shows the electron density enclosed by the H(O) atoms, which is slightly separated from the parent Na atom. Compared with the snapshot at 10.0 ps, less electron density resides near the Na atom at 9.3 ps and is instead associated with several hydroxyl groups that stabilize the electron density in the void space. The electron density is also more localized in the solvation cavity at 9.3 ps than at 10.0 ps. At 9.3 ps, the 0.001 isodensity surface encloses two-thirds of the excess electron within a 28 $Å^3$ volume, whereas a similar fraction is enclosed within 38 $Å^3$ at 10.0 ps. Additionally, the 0.006 isodensity kernel at 9.3 ps encloses 28% of the excess electron within a 3.8 $Å^3$ volume, whereas the 0.006 isodensity surface at 10.0 ps is smaller and encloses only 8% of the electron in 1.2 $Å^3$. Overall, these isodensity surfaces indicate that the electron density is more stabilized and localized away from the Na atom in a solvation cavity at 9.3 ps than at 10.0 ps. Closer inspection reveals that between 9.3 and 10.0 ps, reorientation of the glycerol molecules near the Na atom effectively moves their hydroxyl groups farther away from the ionization region. These fluctuations likely destabilize the cavity around the partially solvated electron and force spin density back toward the ionizing Na.

The Mulliken spin populations in Figure 10 indicate that the trajectory does not follow a steady path toward ionization. In particular, the tendency for the evolving Na^+ and e^- to separate and recombine can be seen in Figure 12, which depicts the spin shift (the distance of separation between Na and the center of the 3s electron density), the Na-atom VDE, and the cluster VIP

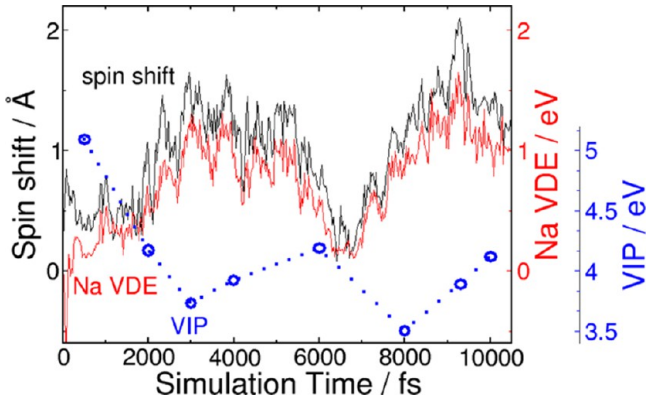

Figure 12. Spin shift, vertical detachment energy (VDE) of the Na atom, and vertical ionization potential (VIP) of the Na/glycerol cluster as functions of simulation time. The spin shift (distance between Na and the center of the excess electron density) correlates well with the Na-atom VDE. The approximate anticorrelation between the VIP and the spin shift indicates that a more separated electron is also more solvated.

over the full 10 ps trajectory. The Na VDE and spin shift track each other well, demonstrating that the separation between the ionizing Na and the electron reports on the solvation of the emerging cation and electron. However, the cluster VIP is approximately anticorrelated with these quantities because the electron becomes less bound as it leaves the Na atom. We do not know why this anticorrelation is not better matched; it may reflect different extents of e^- and Na^+ solvation as ionization progresses. The VIP–spin shift anticorrelation has also been found to be only approximate in previous AIMD simulations of Na ionization in water clusters.[29]

Figure 12 shows that after the Na atom's initial interaction with the cluster at early times, both the Na VDE and the spin

dx.doi.org/10.1021/ja4106144 | J. Am. Chem. Soc. 2014, 136, 3065–3074

shift increase because of concurrent solvation and ionization of the Na atom. Additionally, the cluster VIP decreases from 5 eV (the Na gas-phase ionization energy) and oscillates about ~3.7 eV for the remainder of the simulation. The spin shift and Na VDE reach their maxima at 9.3 ps, consistent with the minimum in Na 3s spin density and maximum ionization of ~80% near this time, as noted above.

As a final means of characterizing the ionization of the Na atom in glycerol, we calculated the electron radius of gyration r_g throughout the simulation using the procedure outlined in ref 65. The radius of gyration is a root-mean-square measure of the size of the electron calculated according to $r_g = [\int s(\mathbf{r})(\mathbf{r} - \mathbf{r}_c)^2 d^3\mathbf{r}]^{1/2}$, where $s(\mathbf{r})$ is the spin density distribution and $\mathbf{r}_c$ is the center of the spin distribution. We found that r_g fluctuates throughout the simulation about a value of 2.5 Å, with a minimum of ~2.3 Å at the point of maximum Na ionization (data not shown). This calculated minimum radius is identical to the value estimated from a moment analysis of the Gaussian–Lorentzian line shape of the optical absorption spectrum of solvated electrons in glycerol at ~300 K.[66,67] The spatial extent of the solvated electron in our simulation thus appears to resemble that observed in bulk glycerol in spite of incomplete ionization and the presence of the Na^+ counterion.

CONCLUSIONS

We have investigated the scattering, uptake, solvation, and ionization of gas-phase sodium atoms striking liquid glycerol with Na atomic beam–surface scattering experiments and ab initio molecular dynamics calculations. The experiments indicate that >75% of the impinging Na atoms disappear into the glycerol film and react with the solvent at $\theta_{inc} = 45°$ and $E_{inc} = 12$ kJ mol^{-1} ($5.0RT_{liq}$). The remaining ~25% of the Na atoms recoil directly from the surface of glycerol with kinetic energies close to that of the incident Na atoms rather than with energies characteristic of thermal desorption. These observations imply that Na-atom thermalization is always followed by irreversible uptake.

The complementary AIMD simulations provide an atomic-scale picture of the short-time behavior of these thermalized Na atoms. Ionization of Na proceeds concurrently with its solvation and begins within 1 ps, providing a means of trapping the Na atom at the surface. Partial and temporary recombination of e^- and Na^+ is seen throughout the simulation, as indicated by the varying Na VDE, cluster VIP, and spin shift. A comparison of the 9.3 and 10 ps simulation snapshots at ~70% and ~30% ionization indicates that fluctuations in the configurations of the glycerol molecules change the solvation of the Na^+ and e^- species and therefore alter the Na^+–e^- separation and extent of ionization.

Although not observed here, we anticipate that longer simulation times and larger cluster sizes would eventually lead to the formation of a fully solvated electron and at much longer times to electron-initiated bond breaking.[64] These reactions were monitored experimentally in an earlier study by recording the evaporation of hydrogen atoms and molecules, water, and solvent fragments upon Na-atom exposure to liquid glycerol.[26] The combined high uptake and reactivity of Na atoms and their rapid ionization upon contact with the glycerol cluster imply that the soft landing of Na atoms on the surfaces of protic liquids may be a general tool for exploring the near-interfacial chemistry of solvated electrons.

AUTHOR INFORMATION

Corresponding Authors

*E-mail: gmnathan@wisc.edu (G.M.N.).
*E-mail: w.alexander@memphis.edu (W.A.A.).
*E-mail: tminton@montana.edu (T.K.M.).
*E-mail: schatz@chem.northwestern.edu (G.C.S.).

Notes

The authors declare no competing financial interest.

ACKNOWLEDGMENTS

This work was supported by the National Science Foundation through Grant CHE-0943639 as part of the Center for Energetic Nonequilibrium Chemistry at Interfaces. W.A.A. is grateful to the Department of Chemistry at The University of Memphis for financial support. We thank Pavel Jungwirth for valuable advice and discussions.

REFERENCES

(1) Hart, E. J.; Anbar, M. *The Hydrated Electron*; Wiley-Interscience: New York, 1970.
(2) Young, R. M.; Neumark, D. M. *Chem. Rev.* **2012**, *112*, 5553–5577.
(3) Abel, B.; Buck, U.; Sobolewski, A. L.; Domcke, W. *Phys. Chem. Chem. Phys.* **2012**, *14*, 22–34.
(4) Turi, L.; Rossky, P. J. *Chem. Rev.* **2012**, *112*, 5641–5674.
(5) Buxton, G. V.; Greenstock, C. L.; Helman, W. P.; Ross, A. B. *J. Phys. Chem. Ref. Data* **1988**, *17*, 513–886.
(6) Spinks, J. W. T.; Woods, R. J. *An Introduction to Radiation Chemistry*, 3rd ed.; Wiley: New York, 1990.
(7) Garrett, B. C.; Dixon, D. A.; Camaioni, D. M.; Chipman, D. M.; Johnson, M. A.; Jonah, C. D.; Kimmel, G. A.; Miller, J. H.; Rescigno, T. N.; Rossky, P. J. *Chem. Rev.* **2005**, *105*, 355–389.
(8) Horio, T.; Shen, H.; Adachi, S.; Suzuki, T. *Chem. Phys. Lett.* **2012**, *535*, 12–16.
(9) Lübcke, A.; Buchner, F.; Heine, N.; Hertel, I. V.; Schultz, T. *Phys. Chem. Chem. Phys.* **2010**, *12*, 14629–14634.
(10) Elles, C. G.; Jailaubekov, A. E.; Crowell, R. A.; Bradforth, S. E. *J. Chem. Phys.* **2006**, *125*, No. 044515.
(11) Zeuch, T.; Buck, U. *Chem. Phys. Lett.* **2013**, *579*, 1–10.
(12) Han, P.; Bartels, D. M. *J. Phys. Chem.* **1992**, *96*, 4899–4906.
(13) Telser, T.; Schindewolf, U. *Ber. Bunsen-Ges. Phys. Chem.* **1984**, *88*, 488–492.
(14) Freeman, G. R. *Actions Chim. Biol. Radiat.* **1970**, *14*, 73–134.
(15) Balaj, O. P.; Siu, C. K.; Balteanu, I.; Beyer, M. K.; Bondybey, V. E. *Int. J. Mass Spectrom.* **2004**, *238*, 65–74.
(16) Barnett, R. N.; Giniger, R.; Cheshnovsky, O.; Landman, U. *J. Phys. Chem. A* **2011**, *115*, 7378–7391.
(17) Siefermann, K. R.; Abel, B. *Angew. Chem., Int. Ed.* **2011**, *50*, 5264–5272.
(18) Siefermann, K. R.; Liu, Y.; Lugovoy, E.; Link, O.; Faubel, M.; Buck, U.; Winter, B.; Abel, B. *Nat. Chem.* **2010**, *2*, 274–279.
(19) Marsalek, O.; Uhlig, F.; VandeVondele, J.; Jungwirth, P. *Acc. Chem. Res.* **2012**, *45*, 23–32.
(20) Sagar, D. M.; Bain, C. D.; Verlet, J. R. R. *J. Am. Chem. Soc.* **2010**, *132*, 6917–6919.
(21) Tang, Y.; Shen, H.; Sekiguchi, K.; Kurahashi, N.; Mizuno, T.; Suzuki, Y.-I.; Suzuki, T. *Phys. Chem. Chem. Phys.* **2010**, *12*, 3653–3655.
(22) Steinbach, C.; Buck, U. *Phys. Chem. Chem. Phys.* **2005**, *7*, 986–990.
(23) Forck, R. M.; Dauster, I.; Buck, U.; Zeuch, T. *J. Phys. Chem. A* **2011**, *115*, 6068–6076.
(24) Kim, J.-H.; Kim, Y.-K.; Kang, H. *J. Phys. Chem. C* **2009**, *113*, 321–327.
(25) Kim, S.; Park, E.; Kang, H. *J. Chem. Phys.* **2011**, *135*, No. 074703.
(26) Alexander, W. A.; Minton, T. K.; Wiens, J. P.; Nathanson, G. M. *Science* **2012**, *335*, 1072–1075.

(27) Burchill, C. E.; Perron, K. M. *Can. J. Chem.* **1971**, *39*, 2382−2389.
(28) Cammenga, H. K.; Schulze, F. W.; Theuerl, W. *J. Chem. Eng. Data* **1977**, *22*, 131−134.
(29) Cwiklik, L.; Buck, U.; Kulig, W.; Kubisiak, P.; Jungwirth, P. *J. Chem. Phys.* **2008**, *128*, No. 154306.
(30) Bonin, J.; Lampre, I.; Pernot, P.; Mostafavi, M. *J. Phys. Chem. A* **2008**, *112*, 1880−1886.
(31) The individual Na^+ and e^- enthalpies of solvation are tethered to the proton enthalpy of solvation. We used the following cycle to obtain the $e^-(g) \rightarrow e_s^-$ enthalpy change: $H(aq) \rightarrow H^+(aq) + e_s^-$, +60 kJ mol^{-1} (ref 33); $H(g) \rightarrow H(aq)$, −4 kJ mol^{-1} (ref 34 using H_2 as a model for H); $H^+(g) + e_g^- \rightarrow H(g)$, −1315 kJ mol^{-1} (ref 32 and the EC-FD electron convention); $H^+(aq) \rightarrow H^+(g)$, +1150 kJ mol^{-1} (ref 35). These steps sum to −109 kJ mol^{-1} for the electron solvation enthalpy at 25 °C. The Na^+ solvation enthalpy of 463 kJ mol^{-1} was determined by a related procedure in ref 35. Lastly, the enthalpy change of −73 kJ mol^{-1} for $Na(g) \rightarrow Na^+(aq) + e_s^-$ was estimated from the sum of −109 and −463 and Na ionization enthalpy of +499 kJ mol^{-1}. This value of −73 kJ mol^{-1} does not depend on the proton enthalpy of solvation or the electron convention.
(32) The Na ionization enthalpy at 25 °C was obtained by adding the EC-FD value of $H(298) - H(0)$ = 3 kJ mol^{-1} for the electron to the ionization energy of Na of 496 kJ mol^{-1}. This correction also applies to H-atom ionization. See: Bartmess, J. E. *J. Phys. Chem.* **1994**, *98*, 6420−6424.
(33) Shiraishi, H.; Sunaryo, G. R.; Ishigure, K. *J. Phys. Chem.* **1994**, *98*, 5164−5173.
(34) Han, P.; Bartels, D. M. *J. Phys. Chem.* **1990**, *94*, 7294−7299.
(35) Tissandier, M. D.; Cowen, K. A.; Feng, W. Y.; Gundlach, E.; Cohen, M. H.; Earhart, A. D.; Coe, J. V.; Tuttle, T. R. *J. Phys. Chem. A* **1998**, *102*, 7787−7794.
(36) Forck, R. M.; Dauster, I.; Schieweck, Y.; Zeuch, T.; Buck, U.; Ončák, M.; Slavíček, P. *J. Chem. Phys.* **2010**, *132*, No. 221102.
(37) Shreve, A. T.; Elkins, M. H.; Neumark, D. M. *Chem. Sci* **2013**, *4*, 1633−1639.
(38) Dauster, I.; Suhm, M. A.; Buck, U.; Zeuch, T. *Phys. Chem. Chem. Phys.* **2008**, *10*, 83−95.
(39) Gao, B.; Liu, Z.-F. *J. Chem. Phys.* **2007**, *126*, No. 084501.
(40) Photodetachment of electrons from anionic clusters is a sudden, vertical process, but electron detachment from Na-doped clusters may be partially adiabatic, as discussed in refs 23, 36, 37, 38, and 39. However, the measured differences in ionization energies between small Na-doped and anionic clusters appear to be much larger than the differences in the experimental and calculated vertical ionization energies of the Na-doped clusters, implying that the Na^+ core stabilizes the excess electron. See Figure 2 in ref 11, Figures 5 and 6 in ref 23, Figure 3 in ref 36, and Figure 6 in ref 38.
(41) Garton, D. J.; Minton, T. K.; Alagia, M.; Balucani, N.; Cassavechia, P. *J. Chem. Phys.* **2000**, *112*, 5975−5984.
(42) Lee, Y. T.; McDonald, J. D.; LeBretron, P. R.; Herschbach, D. R. *Rev. Sci. Instrum.* **1969**, *40*, 1402−1408.
(43) Ringeisen, B. R.; Muenter, A. H.; Nathanson, G. M. *J. Phys. Chem. B* **2002**, *106*, 4988−4998.
(44) Pauly, H. In *Atomic and Molecular Beam Methods*; Scoles, G., Ed.; Oxford University Press: New York, 1988; Vol. *1*, p 83−123.
(45) Blieck, J.; Affouard, F.; Bordat, P.; Lerbret, A.; Descamps, M. *Chem. Phys.* **2005**, *317*, 253−257.
(46) Cornell, W. D.; Cieplak, P.; Bayly, C. I.; Gould, I. R.; Merz, K. M.; Ferguson, D. M.; Spellmeyer, D. C.; Fox, T.; Caldwell, J. W.; Kollman, P. A. *J. Am. Chem. Soc.* **1995**, *117*, 5179−5197.
(47) Chelli, R.; Procacci, P.; Cardini, G.; Califano, S. *Phys. Chem. Chem. Phys.* **1999**, *1*, 879−885.
(48) Ponder, J. W.; Richards, F. M. *J. Comput. Chem.* **1987**, *8*, 1016−1024.
(49) Baldelli, S.; Schnitzer, C.; Schultz, M. J.; Campbell, D. J. *J. Phys. Chem. B* **1997**, *101*, 4607−4612.
(50) Oh-e, M.; Yokoyama, H.; Baldelli, S. *Appl. Phys. Lett.* **2004**, *84*, 4965−4967.
(51) Benjamin, I.; Wilson, M.; Pohorille, A. *J. Chem. Phys.* **1994**, *100*, 6500−6507.
(52) VandeVondele, J.; Krack, M.; Mohamed, F.; Parrinello, M.; Chassaing, T.; Hutter, J. *Comput. Phys. Commun.* **2005**, *167*, 103−128.
(53) Rettner, C. T.; Schweizer, E. K.; Mullins, C. B. *J. Chem. Phys.* **1989**, *90*, 3800−3813.
(54) Alexander, W. A.; Zhang, J. M.; Murray, V. J.; Nathanson, G. M.; Minton, T. K. *Faraday Discuss.* **2012**, *157*, 355−374.
(55) After 8 h of beam exposure to an FEP Teflon sheet, a black spot roughly matching the projected Na beam spot could be seen on the sheet. Upon sample exposure to air, the spot turned white, which is consistent with the formation and decomposition of an unstable carbyne product observed previously (ref 56). This 8 h exposure corresponds to $\sim 10^{20}$ Na atoms cm^{-2}. The Teflon monomer unit density is $\sim 10^{22}$ cm^3. If each Na atom reacts by removing one monomer unit, then the Na atoms would have etched a depth of 100 μm into the Teflon sample. The etched depth was not precisely measured but was less than 1 μm, corresponding to a reaction probability of less than 1%. This loss in the scattered Na atom flux from Teflon would raise the lower limit for the Na−glycerol uptake probability of 0.75 by less than 0.01. However, on the basis of our previous experience with more highly reactive O-atom etching of fluorinated polymers, it is likely that more than one Na atom must react to remove a Teflon monomer. In this case, the Na−glycerol uptake probability would be even larger.
(56) Soneda, Y.; Maruoka, K.; Nakano, M.; Akuzawa, N.; Yamada, Y. *Proc. ADC/FCT* **1999**, 571.
(57) Rendulic, K. D.; Winkler, A. *Surf. Sci.* **1994**, *299*, 261−276.
(58) Rettner, C. T.; Auerbach, D. J. *Science* **1994**, *263*, 365−367.
(59) Humphrey, W.; Dalke, A.; Schulten, K. *J. Mol. Graphics* **1996**, *14*, 33−38.
(60) Frigato, T.; VandeVondele, J.; Schmidt, B.; Schutte, C.; Jungwirth, P. *J. Phys. Chem. A* **2008**, *112*, 6125−6133.
(61) The maximum ionization of 78.1% was found at 9.283 ps, while the ionization at 9.300 ps was 69.5%.
(62) Zhuang, W.; Dellago, C. *J. Phys. Chem. B* **2004**, *108*, 19647−19656.
(63) Geissler, P. L.; Dellago, C.; Chandler, D.; Hutter, J.; Parrinello, M. *Science* **2001**, *291*, 2121−2124.
(64) We estimate a $\sim$10 μs or shorter time for reaction of solvated electrons with glycerol solvent using information in ref 26, which suggests that D atoms created by the electrons react with d_8-glycerol molecules throughout a depth (z) of $\sim$50 Å. This depth is traversed by electrons over a time of $z^2/D \approx 10^{-5}$ s, where $D \approx 3 \times 10^{-8}$ cm^2 s^{-1} for electron diffusion in glycerol.
(65) Marsalek, O.; Uhlig, F.; Jungwirth, P. *J. Phys. Chem. C* **2010**, *114*, 20489−20495.
(66) See eq 10 in the following reference: Coe, J. V.; Williams, S. M.; Bowen, K. H. *Int. Rev. Phys. Chem.* **2008**, *27*, 27−51.
(67) Bartels, D. M. *J. Chem. Phys.* **2001**, *115*, 4404−4405.